ICAS-98-2,10,1

MODELING EXHAUST JET DILUTION IN AIRCRAFT WAKES: APPLICATION TO CONTRAIL FORMATION

F. Garnier and A. Laverdant

Office National d'Etudes et de Recherches Aérospatiales (ONERA), Châtillon, France

Abstract

In order to investigate the process of contrail formation, an integral model and a two-dimensional direct numerical simulation have been performed to analyze the mixing and entrainment processes of the engine exhaust through their interaction with the vortex wake of various aircraft. The objective of this study is to evaluate the partial vapor pressure of water and temperature in the nearfield of subsonic and supersonic aircraft. Results are presented involving the relative humidity calculation by post-processing solution fields and provide a qualitative indicator of the condensation process.
After testing numerical algorithm with some success, this study was performed for three transport subsonic aircraft: A-330, B-737 and DC-9; for twin-engine ATTAS of DLR and for the Anglo-French supersonic Concorde.

For subsonic aircraft, in the early wake, the distance where the saturation is reached depends only upon the engine jet characteristics. For the supersonic aircraft, a low relative humidity has been shown in the plume centerline. However, the wing-tip vortices contributes largely to increase the mixing and dispersion of the exhaust plume. Consequently the persistence or evaporation processes is clearly changed by the vortical structure. Effects of aerodynamics parameters are analyzed and discussed.

1. Introduction

The future built-up of a large fleet of commercial aircraft, subsonic and supersonic, may provide a major atmospheric perturbation for the next decades. One critical point of the impact of aircraft emissions upon the atmosphere concerns the effect of aircraft exhaust on aerosol and cloud formation. These exhaust emissions contain mainly water vapor, carbon oxide, unburned hydrocarbons and minor gases, due to the high combustion efficiency. Recent study[1] has shown the important role of the water vapor-sulfuric acid system on aerosol formation in the wake. For favorable ambient relative humidity and temperature, typically colder than -40°C, these emissions can lead to ice nucleation and growth processes that will form condensation trails or contrails. However contrails may also form at higher temperature, above 0°C, when humid air expands around the aircraft. It can condense and illustrate certain flow patterns such as the top of the wings of the Concorde during landing[2].

Even if the direct effects of the water vapor emissions seem negligible, the role in the Earth's radiative budget of the droplets and of the particles emitted by the jet engine remains unclear and needs more studies [3-4]. The recent conclusions[5] pointed out the great uncertainty concerning the role on cloud formation of contrails created by aircraft at the local scale *i.e.* at the vortex wake scale. This mainly includes the knowledge of the mixing and condensation processes in the aircraft wake.

The wake of an aircraft is composed of two counter-rotating wing-tip vortices. The vortical motion is generated by strong radial pressure gradients. As shown by Ehret and Ortel[6] the engine jets are initially virtually insensitive to the details of the vortex flow and later the exhaust emissions are captured by the vortices.
The details of the mixing process are complicated and result of different proceeds. It is useful to define three regions. Firstly, the nearfield jet regime is characterized by physical processes of usually co-flowing jets. Secondly the deflection regime corresponds to the entrainment of the jet engine towards the vortex core and finally the shearing regime where the jet streamlines present distortion and stretching generated by the rotational component of the velocity inside the vortex cores. For modern large transport aircraft, they describe the jet evolution over the time periods of approximately, 0-1 s, 1-5 and 5-30 s after the release of the hot jet from the nozzle exit into the atmosphere.
The effect of trailing vortices on the dilution and chemistry of the exhaust jets has been studied by several authors[7-8-9]. In the present study we focus on a simplified

analysis based on the problem of the interaction between an interface (*i.e.* shear layer of the exhaust jet flow) and a vortex. This approach is at the origin of a lot of works, for example, for a flame vortex interaction[10] and for the mixing between two media[11]. In this last case, the problem can be simply described by a convection-diffusion equation for the passive scalar. The Péclet number is the parameter, used in this simulation. The flow field is approximated by an analytical solution of the Navier-Stokes equations.

The objective of this work is to assess the accurate partial pressure of water and temperature in the near-field of the vortex wake. For assessing these locals variables which control the dispersion and dilution of the aircraft emissions, an integral model and a two-dimensional direct-simulation of convection-diffusion equation have been developed. Results are presented involving the relative humidity calculation by post-processing solution fields and provide a qualitative indicator of the condensation process.

2. Numerical models

Our first aim is to characterize the mixing process produced by the interaction between engine jets and vortex wake. A schematic representation of this mechanism is represented in Figure 1. An integral model has been used to take continuously into account the jet mixing during the first two regimes described above, *i.e.* up to its entrainment into the vortex core. This approach is described in a Lagrangian framework and uses the control volume concept to integrate the conservation laws of mass, momentum and energy. The vortex wake is represented by the superposition of two Gaussian vortices. The turbulent diffusion and its effect on the expansion and cooling of the jet are based on the Morton-Taylor-Turner analysis. This approach is generalized to account for the transversal shear generated by the vortical motion[12].
Change in the mean concentration of a tracer in a jet is intimately tied to the rate of entrainment, i.e. the rate at which vortical ambient fluid is included within the jet boundaries. The expression of the entrainment function writes:

$$E = \tilde{\rho}\left[\alpha_s\left(V_s - \tilde{V}_s\right) + \alpha_n\sqrt{\tilde{V}_n^2 + \tilde{V}_b^2}\right]D \qquad (1)$$

where subscript *s*, *n* and *b* denote respectively the velocity components tangential, normal and binormal to the jet path; D the jet diameter and ρ the density. The tilde is referenced as the ambient fluid. The coefficients α_s and α_n are empirical constants[13].

After the integral model run, the transport and the mixing of the plume has been studied by means of the convection-diffusion equation in an Eulerian framework.
The flow field examined here consists of a pair of two-dimensional Lamb-Oseen viscous core vortices. Note, that, from this work, a three-dimensional velocity field can be introduced, Batchelor has proposed an elegant solution with a simple form (the q-vortex)[14]. The problem is well posed when the flow velocity, the boundary and initial conditions are imposed. A quantitative analysis of mixing is given in terms of calculation of dilution ratio *Z* (or the mixture variable) and mixedness *f* which is defined by the following relation:

$$f = \frac{4}{S}\int_S Z(1-Z)dS \qquad (2)$$

where *S* represents the area of the domain, which is selected here to allow comparisons of the mixedness for various aircraft wakes. This parameter has a finite value since the far field of the vortex wake is surrounded by normalized concentrations at Z=0. In a given domain the value of *f* varies between 0 for completely unmixed region (*i.e.* ambient air) and 1.0 for the Gaussian plume. Then the equation for *Z* can be written in a dimensionless form (denoted by a star) and takes the expression given by:

$$\frac{\partial Z}{\partial t^*} + U^*\frac{\partial Z}{\partial X^*} + V^*\frac{\partial Z}{\partial Y^*} = \frac{1}{\mathrm{Re}\,Sc}\left(\frac{\partial^2 Z}{\partial X^{*2}} + \frac{\partial^2 Z}{\partial Y^{*2}}\right) \qquad (3)$$

where *Re* and *Sc* represent respectively the Reynolds and Schmidt number ($Sc = \upsilon/D$). Note that Péclet number *Pe* can be defined from *Re* and *Sc*: $Pe = Sc\,Re$. U^* and V^* are the Cartesian velocity coordinates, determined from the tangential velocity for viscous core vortices.

At first glance, this problem seems easy to solve but it is not so. A simple test consists in solving the one dimensional convection equation with constant velocity (infinite Péclet number). In that case, the solution is obvious: the initial profile is identically convected. Numerical tests show that some schemes present oscillations (2 nd order) or overdiffuse (1st order)[15-16-17]. This flaw can be eliminated by the introduction of flux limiters. Many new schemes are proposed, but one dimensional tests show that for the convection of a square wave, a Gaussian or a half dome, remarkable dumping are observed (particularly for the Gaussian wave). This last test is well solved with the F.C.T. algorithm[18]. The scheme comports a monotone scheme (upwind) and a high order centered scheme (4th, 6th; 8th or 16th order). The flux limiter suppresses numerical oscillation, which are observed far from these discontinuities.

In the present work, the Zalesak scheme of 8th order in space is retained. The time integration is made with a 3rd order Runge-Kutta[19]. The results are similar to the one obtained with the classical 4th order Runge-Kutta scheme. Many tests have been made (data not shown). As an example, we present one of the most severe test for a two dimensional geometry which is the solid body rotation of a slotted cylinder. The velocity field in Cartesian coordinates takes this simple form:

$$\begin{cases} u = -\Omega(y - y_0) \\ v = \Omega(x - x_0) \end{cases} \qquad (4)$$

where Ω is the constant angular velocity in rad/s; x_0, y_0 define the position of the rotation axis. The grid is regular (100 x 100). The rotation, which is counter-clockwise, is centered on the domain center. The time step and the angular velocity are taken in a manner that 628 time steps give a complete rotation.

The initial condition for the slotted cylinder is plotted in Figure 2. The passive scalar takes a value of 3 inside the cylinder whilst it is zero in the slot and outside. The final result is plotted, not at the same scale, in Figure 3. The back of the cylinder has fallen and slight perturbations are observed in the slot. However, the slot is not full. The present results are similar to the ones obtained by Zalesak.

The numerical simulation of the plume mixing is performed for a laminar case, using a Péclet number (or Reynolds number since we will take Sc=1.) based on the vortices strength and equal to 3000. Turbulence mixing is suppressed by rotation. However the decay of the wake strength is driven by ambient turbulence to gradually cause the destruction of the vortex wake by Crow instability[20].

3. Relative humidity principle

Wing tip vortices interact with ambient medium and plume exhaust in which they exist in that they may change substantially the fluid properties. The most well known form of such interaction is the condensation trail or " contrail ". Detailed modeling of the exact condensation process is beyond the scope of this current work. However, relative humidity is used as a qualitative indicator of where the wake flow is likely to begin to condense ($RH \geq 1$) and where the contrail will form. So, in the trailing vortices, any small particles, such as for example soot release by engines of aircraft, will provide the seed particles for condensation process to occur. This mechanism is complex and is not taken into account in the present analysis. It includes many processes such as binary homogeneous and heterogeneous nucleation on pre-existing particles[21], mainly soot and atmospheric dust trapped by the vortex system.

The objective of this section is to obtain an expression for local relative humidity as a function of dilution ratio Z that is computed by the convection-diffusion code described in the previous section. This includes atmospheric values of static pressure, temperature and relative humidity.

To introduce a general approach, the flow field is considered here as a mixture of two gases, having uniform properties over one part of the flow field, which is called the plume stream (maximum water content), and different uniform properties over the atmospheric flow stream.

Let define relative humidity for ambient stream:

$$RH_a = \frac{F_{H2O,a} P_a}{P_{s,a}} \qquad (5)$$

Similarly, for plume flow:

$$RH_p = \frac{F_{H2O} P_a}{P_{s,p}} \qquad (6)$$

where P_a represents the static pressure at flight altitude which has the same value in the plume flow (isobaric conditions). $P_{s,a}$ and $P_{s,p}$ are respectively the pressure of saturated H_2O vapor for ambient medium and plume stream. They are obtained from Tabata's expression[22]. $F_{H2O,a}$ and F_{H2O} are respectively the H_2O mixing ratio of atmospheric medium and plume flow. Furthermore the value of F_{H2O} depends on the calculation of the dilution ratio Z and can be given by the following expression:

$$F_{H2O} = F_{H2O,a} + Z(F_{H2O,j} - F_{H2O,a}) \qquad (7)$$

where $F_{H2O,j}$ is the H_2O mixing ratio at the nozzle exhaust.

If one assumes that the density variations associated to the latent heat release, due to phase change, are neglected, a similar expression can be written for the temperature field T:

$$T = T_a + Z(T_j - T_a) \qquad (8)$$

where T_a and T_j are respectively the atmospheric and nozzle exhaust temperatures.

4. Initial conditions and field data

As recalled in section 2, the aircraft produces a vortex wake compounded by two rolled-up vortices of opposite circulation $\pm\Gamma$ and spacing $\tilde{b}$ (see Figure 4), the aerodynamic parameters of various aircraft and flight conditions, used for numerical simulations, are described in Table 1. For subsonic aircraft; A-330, B-737, DC-9 and ATTAS, the flight conditions are given by the AEROCONTRAIL European project. Its objective is to provide a better understanding on aerosol and cloud formation and of their impact on the climate, measurements of $H_2O_{(g)}$ mixing ratio in the atmosphere have been obtained and partially given in Table 1.

Schumann et al.[23] published results of the contrail formation in the exhaust plume for the DLR's ATTAS aircraft. Details of the near field flow properties described in this work, have been used to calculate the mixing (*i.e.* the dilution ratio) throughout the wake.

ZEBRA campaign was devoted to observations of the contrail of Concorde, flying into the polar vortex at supersonic speed close to the town of Andoya in Norway.

Although most of the emphasis was to study the ice crystals formation through which ozone destruction could be occured, details of the dilution evolution inside the vortex wake has been performed by models[24]. The initial data used for this calculation are given in the last column of Table 1.

The calculations for large subsonic (*i.e.* except for ATTAS aircraft) and supersonic aircraft have been carried out simulating respectively a CFM-56 engine and an OLYMPUS engine.

5. Results and discussion

Figure 5 shows the mixedness parameter as a function of plume age for three subsonic aircraft. This parameter is calculated using laminar DNS approach, where the dilution ratio is convected and diffused into the wake vortex. Mixedness increases with plume age and its rate of change becomes weaker with increasing time. The intensitivity of the rate of mixing depends on the manner in which the exhaust plume and the vortical structures are initiated. This includes various parameters, such as plume diameter, its relative location with respect to the vortex axis, Péclet number and aircraft characteristics. Finally, it

	Airbus A-330	Boeing B-737	Douglas DC-9	Fokker ATTAS	Concorde
Ambient Temperature (K)	220	220	220	220	202
Ambient pressure (hPa)	288	288	288	288	90
Ambient $H_2O_{(g)}$ mixing ratio	$1.217\ 10^{-4}$	$1.217\ 10^{-4}$	$1.217\ 10^{-4}$	$1.217\ 10^{-4}$	$3.5\ 10^{-6}$
Aircraft weight (N)	$2.08\ 10^{6}$	$4.9\ 10^{5}$	$4.5\ 10^{5}$	$1.9\ 10^{5}$	$1.5\ 10^{6}$
Span b (m)	60.3	28.88	28.47	21.5	25.56
Aspect ratio	9.3	7.9	8.71	7.22	1.825
Wing surface (m^2)	361.3	105.4	92.97	64.	358.
Circulation Γ (m^2s^{-1})	540.	195.	252.	150.	625.
Aircraft velocity (ms^{-1})	252.	240.	240.	163.	570.
Distance engine/wing-tip (m)	21	9.4	11.67	7.8	7.22
Nozzle diameter primary flux (m)	0.61	0.61	0.61	0.707	1.76
Jet exhaust velocity (m/s)	480.3	480.3	480.3	482	1031
Jet exhaust temperature (K)	580.	580.	580.	624	500
Exhaust $H_2O_{(g)}$ mixing ratio	0.035	0.035	0.035	0.035	0.026

Table 1 Aerodynamic parameters, thermodynamic conditions at the exit of engines and flight conditions used as initial parameters for the simulations of several subsonic and supersonic aircraft.

shows that the effect of entrainment and mixing processes in the nearfield jet and deflection regimes dominates the start-up value of the dilution but has a weak influence on its evolution in the shearing regime.

Figure 6 and 7 present the relative humidity or water saturation ratio versus wake age for subsonic A-330 aircraft. These results are obtained when considering an isolated jet flow (*i.e.* without the action of the wing-tip vortices) and an interaction with the two wing-tip vortices. For this aircraft, profiles are shown for the plume axis and an average value inside the plume exhaust. Comparison (see Figure 6) shows that the action of vortical structure decreases the distance where the saturation (RH or $P/P_0 = 1.0$) is reached and only along the plume axis. Accounting for the interaction of vortices, saturation is reached at about 0.8 s plume age (or 190 m downstream of the nozzle exhaust). With an axisymmetric co-flow assumption, saturation is obtained at about 1.2 s or 300 m along the plume axis. For the plume mean value the saturation is reached at about 0.22 s (about 55 m, *i.e.* less than a wing-span for an A-330 aircraft) in the two cases (mean and maximum values). The persistence or evaporation process is clearly changed by the vortical structure. However as the evaporation process is not exactly detailed, these results are only qualitative. Furthermore, as evaporation does not occur, persistent contrails form when the atmospheric environment is supersaturated with respect to ice. This is ignored in the present analysis.

Figure 8 shows a contrail photograph behind a four engine jet aircraft[25]. It forms early after the aircraft, in the co-flowing jet regime. Comparison with the computed relative humidity (see Figure 6) gives the same order of magnitude for the distance where the saturation is reached, and for the distance where the contrail will appear, *i.e.* between 30-60 meters downstream of the exit plane of the engine.

Figure 9 and 10 depict the relative humidity profiles versus wake age, computed for subsonic aircraft. Only the mean values are presented. For all large transport aircraft, A-330, B-737 and DC-9, the distance where the saturation appears is the same. This is explained by the fact that the contrail formation region takes place in the jet regime, less than 1 s plume age, and only the engine jet characteristics control the distance where the saturation occurs. At this early time the action of wing-tip vortices is not efficient. However persistent trails depends on the aerodynamic parameters of the aircraft: wing span, vortex circulation, position of the engine with respect to the wing-tip. It is shown by the slump of the saturation profiles at about 2 s, 3 s and 4.2 s age plume for the B-737, DC-9 and A-330 respectively. At this stage, the entrainment and mixing processes is dominated by the stretching and the distortion of the interface between exhaust plume and ambient air. Then, the evaporation process is only due to laminar diffusion of temperature and water vapor.

Figure 10 shows that for the ATTAS aircraft, the saturation is reached earlier (about 45 m) than the large subsonic aircraft A-330. Change in the mean relative humidity is intimately related to the rate of entrainment, *i.e.* the rate at which ambient fluid is included within the jet boundaries or interface. Therefore, in the jet flow regime, a similarity parameter can be introduced to characterize the entrainment or expansion mechanism. It is defined as the following ratio R:

$$R = \frac{(1-\frac{V_p}{V_a})(1+\sqrt{\frac{\rho_p}{\rho_a}})}{1+\frac{V_p}{V_a}\sqrt{\frac{\rho_p}{\rho_a}}} \qquad (9)$$

where V_p and V_a represent the velocities of the plume flow and the aircraft respectively. We use a similar definition for the density ρ.

In the jet phase, we propose to use an expansion law of the plume diameter D as a linear function of the

axial distance x and the ratio R: $D(x) \approx 0.1Rx$ [26]. From the conservation of mass the plume diameter D can be expressed as a function of the dilution ratio Z and the ratio of velocities and densities:

$$S = \frac{\pi}{4}D^2 = Z\left(\frac{V_a}{V_p}\right)\left(\frac{\rho_a}{\rho_p}\right)\frac{\dot{m}_j}{\rho_a V_a} \qquad (10)$$

where $\dot{m}_j$ is the plume flow rate at the exit nozzle, defined from the engine characteristics (see table 1).

Finally from equation (7) and (8), it can be seen that the relative humidity expression can be written as a function of the ratio $\frac{V_p}{V_a}$ and $\frac{\rho_p}{\rho_a}$. That means that the gap between the different relative humidities computed (see Figure 10) is mainly due to the difference between the ratio of aircraft and plume velocities (see table 1). The ratio of the densities are nearly similar for the two aircraft engines and do not have significant effect on the calculation of the *RH* parameter.

Figure 11 shows the *RH* profiles as a function of plume age for the Concorde. Profiles are presented for the plume axis and for a mean value in the plume. For the mean value, the saturation is reached at about 0.2 s plume age (or ~ 115m downstream of the nozzle exit). However the relative humidity parameter does not reach 1.0 in the plume centerline even at 0.4 s (or ~230 m downstream). The experimental data provided by ZEBRA experiment are in good agreement with the simulation (data not shown) and the distance where the saturation is obtained is accurately predicted by the models. In addition, to test the efficiency of the dilution evolution computed throughout the wake of the Concorde, available experimental data have been obtained during the ASHOE/MAESA campaign (see Figure 12). The Airborne Southern Hemisphere Ozone Experiment (ASHOE) has been conducted in concert with the campaign, Measurement for Assessing the Effects of Stratospheric Aircraft (MAESA). The white squares in Figure 12 show the CO_2 data. The extrapolation of our modeling results (white triangles and circles) compared to the experimental data seems to be acceptable. For comparison, results of a different analysis carried out by Miake-Iye et al.[27] have been plotted (black squares in Figure 12). The better agreement is found in the jet regime up to 0.15 s plume age. In the shearing regime the discrepancy increases but the model results are of the same order of magnitude.

6. Conclusion

Modeling of contrail formation and persistence depend mainly on the knowledge of accurate partial vapor pressure of water and temperature fields throughout the vortex wake and environment medium.

The objective of this paper is to analyze the mixing and dispersion of the exhaust plume in the nearfield of various aircraft through the dilution ratio evaluation. For assessing this passive scalar (considered as a tracer concentration) an integral model and a two-dimensional direct simulation of convection-diffusion equation have been used.

The test of the numerical algorithm, made with some success, has permitted us to investigate a situation of practical interest, *i.e.* the problem of an interaction between a jet interface and a vortex.

Although the detailed modeling of the exact condensation is beyond the scope of this analysis, the water saturation profiles are accurately obtained for subsonic and supersonic aircraft. The relative humidity calculations should prove to be good indicators of the downstream distance of the exit nozzle where the saturation is reached. Water saturation ratio computed for subsonic aircraft shows that the contrail formation region takes place in the coflowing jet and depends mainly on the parameters of engine exhaust jet. However the persistence and evaporation processes are clearly modified by the vortical structures.

For supersonic aircraft, a low relative humidity is obtained for the plume centerline. In this case, the action of the vortices contributes to increase the distance where the saturation appears.

We show that the mixing of the exhaust plume depends strongly on the relative location of the engine with respect to vortex axis and on the vortex strength. However the mixing process was shown to be substantially affected by these parameters in the shearing regime, where the shape of the interface between plume and ambient air is submitted at a stretching and a distortion.

For supersonic aircraft, tracer concentration profiles obtained from various analyses: UNIWAKE code and the present approach, show good agreement with the experimental data.

---

[1] Taleb D.E., Ponche J.L., Mirabel P., Vapor pressures in the ternary system water-nitric acid-sulfuric acid at low temperature: A reexamination, Journal of Geophysical Research, 101, 25,967-25,977, (1996).

[2] Campbell J.F., Chambers J.R. and Rumsey C.L., Observation of airplane flowfields by natural condensation effects, Journal of Aircraft, 26, 7, 593-604, (1989).

[3] Fortuin J.P.F., Van Dorland R., Wauben W.M.F. and Kelder H., Greenhouse effects of aircraft emissions as calculated by a radiative transfert model, Annales Geophysicae, 13, 413-418, (1995).

[4] Ponater, M., S. Brinkop, R. Sausen, and U. Schumann, Simulating the global atmospheric reponse to aircraft water vapour emissions and contrails: a first approach using a GCM, Annales Geophysicae, 14, 941-960, (1996).

[5] Impact de la flotte aérienne sur l'environnement atmosphérique et le climat, French Academy of Sciences, Paris, 40, (1997).

[6] Ehret T. and Oertel H., Numerical simulation of the dynamics and decay of trailing vortices including pollutants from air traffic, Conf. Proc., Impact of emissions from aircraft and spacecraft upon the atmosphere. DLR Mitteilung 94-06, Köln, 268-273, (1994).

[7] Anderson M.R., Miake-Lye R.C., Brown R.C., and Kolb C.E., Numerical modeling of reacting engine plumes and aircraft wake interactions, AIAA paper, 96-0948, (1996).

[8] Kärcher B., Transport of exhaust products in the near trail of a jet engine under atmospheric conditions. Journal of Geophysical Research, 99, 14509-14517, (1994)

[9] Garnier F., Baudoin C., Woods P., Louisnard N., Engine emission alteration in the near field of an aircraft, Atmospheric Environment, 31, 12, 1767-1781, (1997).

[10] Laverdant A.M., Candel S.M., Computation of diffusion and premixed flames rolled-up in a vortex structure, Journal of Propulsion and Power, 5, 2, 134-144, (1989).

[11] Cetegen B.M., Mohamad N., Experiments on liquid mixing and reaction in a vortex, Journal of Fluid Mechanics, 249, 391-414, (1993).

[12] Garnier F., Brunet S., Jacquin L., Modelling exhaust plume mixing in the near field of an aircraft, Annales Geophysicae, 15, 1468-1477,(1997).

[13] Jacquin L., Garnier F., On the dynamics of engine jets behind a transport aircraft, Conference proceedings, AGARD-584 FDP Symposium, The characterisation & modification of wakes from lifting vehicles in fluids. (1996).

[14] Batchelor G.K., Axial flow in trailing line vortices, Journal of Fluid Mechanics, 20, 4, 645-658 (1964).

[15] Boris J.P., Book D.L., Flux-Corrected Transport III. Minimal-error FCT algorithms, Journal of computational physics, 20, 397- 431 (1976).

[16] Book D.L., Boris J.P., Zalesak S.T., Flux-Corrected Transport, in Finite-difference Techniques for Vectorized Fluid Dynamics Calculations, Book, D. (*ed.*), Springer-Verlag, Berlin, (1981).

[17] Oran E.S., Boris J.P., Numerical simulation of reactive flows, Elsevier, London, (1987).

[18] Zalesak S.T., Fully multidimensional flux-corrected transport algorithms for fluids, Journal of computational physics, 31, 335-362 (1979).

[19] Shu C.W. et Osher S., Efficient Implementation of Essentially Non-oscillatory Shock-Capturing Schemes, Journal of Computational Physics, 77, 439-471, (1988).

[20] Spalart P.R., Airplane trailing vortices, Annual Review Fluid Mechanics, In press, (1998)

[21] Brown R.C., Miake-Lye R.C., Anderson M.R, Kolb C.E. and Resh T.J., Aerosol dynamics in near field aircraft plumes. Journal of Geophysical Research, 101, 22,939-22,953, (1996)

[22] Tabata S., A simple but accurate formula for the saturation vapor pressure over liquid water, Journal of Applied Meteorology, 12, 1410-1412, (1973)

[23] Schumann U., Ström J., Busen R., Baumann R., Gierens K., Krautstrunk. M., Schröder F.P. and Stingl J., In situ observations of particles in jet aircraft exhausts and contrails for different sulfur-containing fuels, Journal of Geophysical Research, 101, 6853-6869, (1996)

[24] Nardi B., Pommereau J.P., Hauchecorn, Garnier F., Louisnard N., Taleb D., Mirabel P., Impact of SST water vapor emission in the arctic winter stratosphere: the ZEBRA Concorde experiment, submitted to Journal of Geophysical Research, (1998).

[25] Schumann U., Contrail formation from aircraft exhausts, Meteorol. Zeitschrift, 5,4-23, (1996).

[26] Papamoschou D. and Roshko A., The compressible turbulent shear layer: an experimental study, Journal of Fluid Mechanics, 197, 453-477 (1988).

[27] Miake-lye R.C., Anderson M.R., Brown R.C., and Kolb C.E., Calculation of wake structure and emissions of the Concorde, 5th Annual Meeting on Atmospheric Effects of Aviation Project, Virginia Beach, V.A.

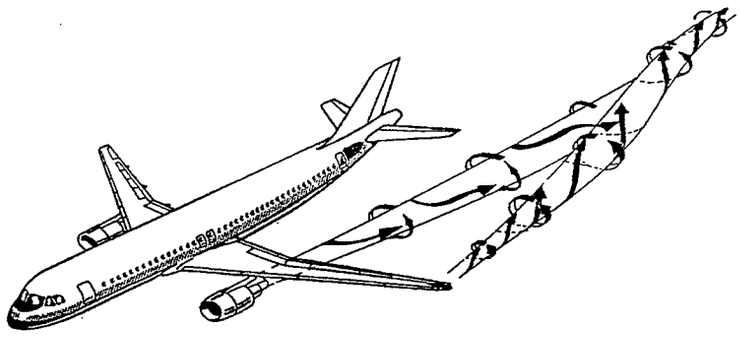

Figure 1: Schematic view of the interaction mechanism of the jet engine with the wing-tip vortices.

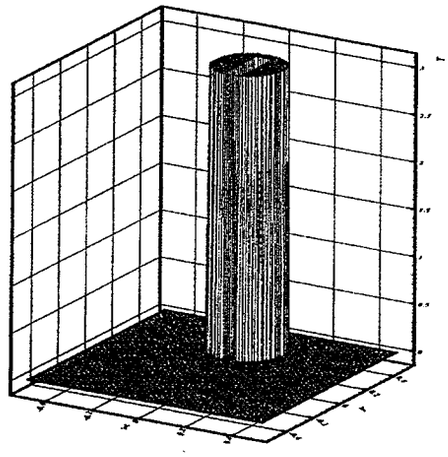

Figure 2: Perspective view of initial condition for the 2-D solid body rotation problem.

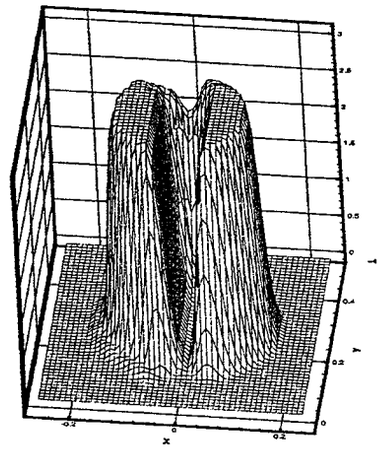

Figure 3: Perspective view of the passive scalar Z for the solid body rotation after 628 cycles (1 revolution).

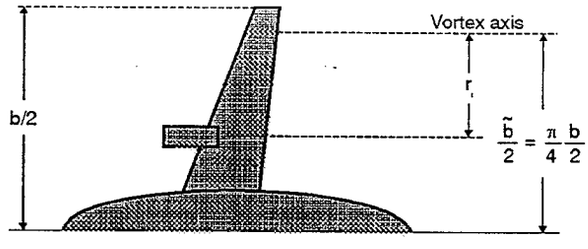

Figure 4: Schematic representation of the engine jet locations.

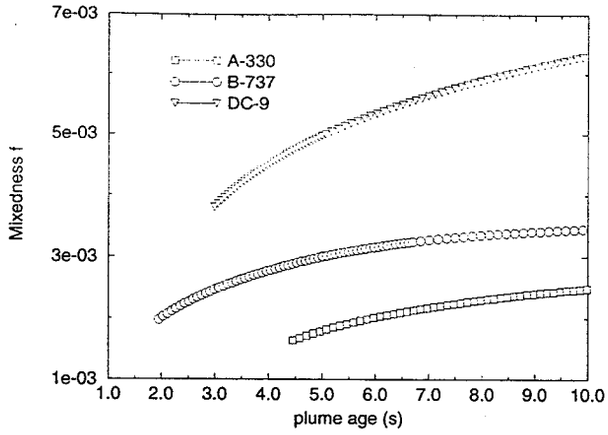

Figure 5: Mixedness as a function of plume age for large subsonic aircraft. Results are computed from a direct numerical simulation of a convection-diffusion equation.

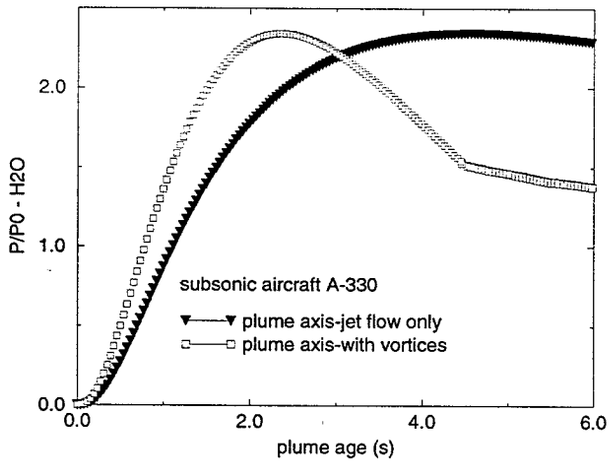

Figure 6: Effect of the wing-tip vortices on the relative humidity $RH = P/P_0$, as a function of plume age, for an A-330. Results are shown for the plume centerline.

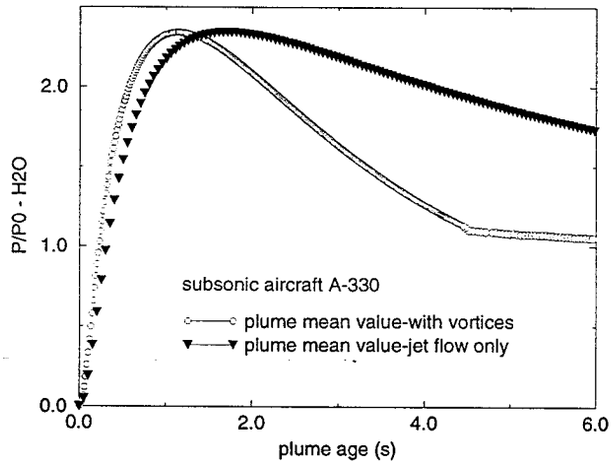

Figure 7: Effect of the wing-tip vortices on the relative humidity $RH = P/P_0$, as a function of plume age, for an A-330. Results are shown for an average value inside the plume exhaust.

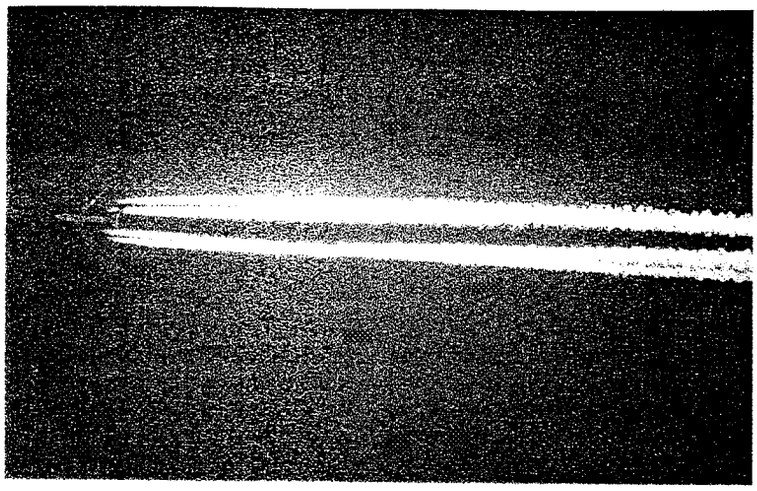

Figure 8: Contrail photograph of a large transport aircraft.

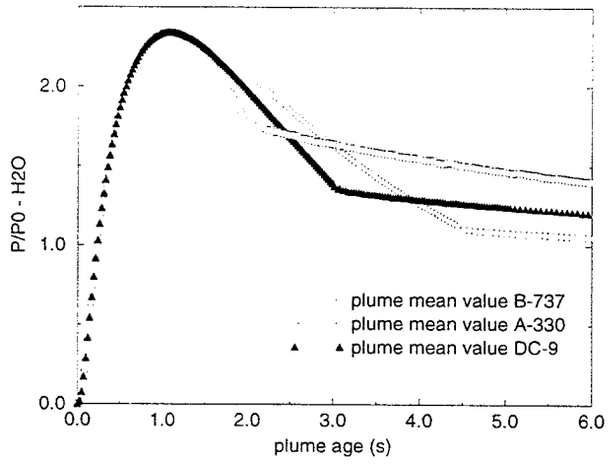

Figure 9: Comparison of water saturation ratio for large subsonic aircraft versus plume age.

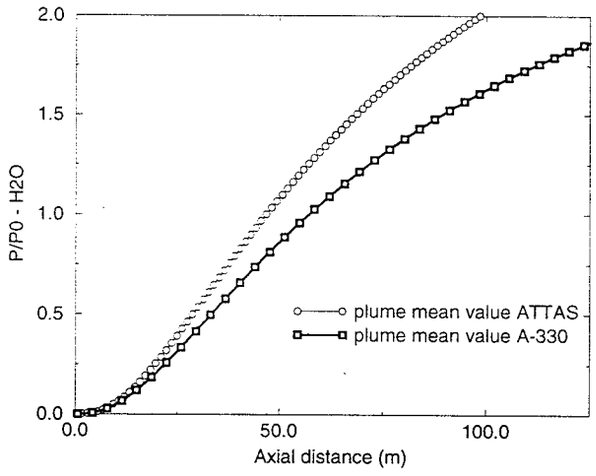

Figure 10: Water saturation ratio $RH = P/P_0$ as a function of axial distance for an A-330 and an ATTAS. Results are shown for an average value inside the plume exhaust.

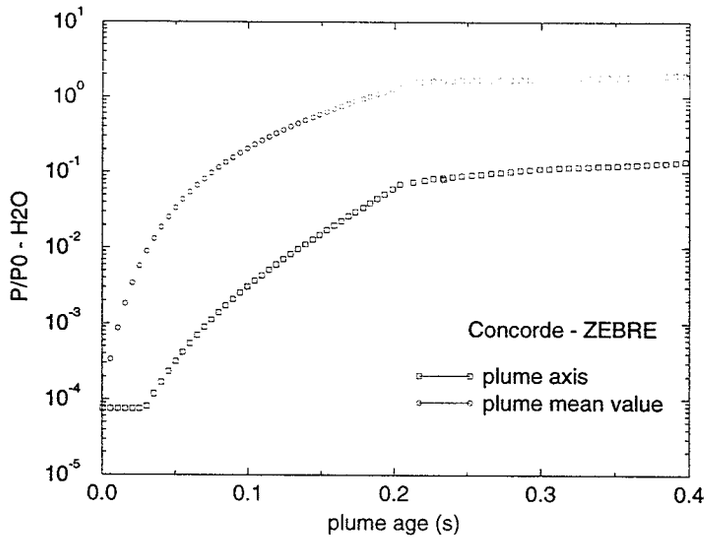

Figure 11: Water saturation ratio $RH = P/P_0$ as a function of plume age for Concorde supersonic aircraft. Results are shown for the plume centerline and for an average value inside the plume exhaust.

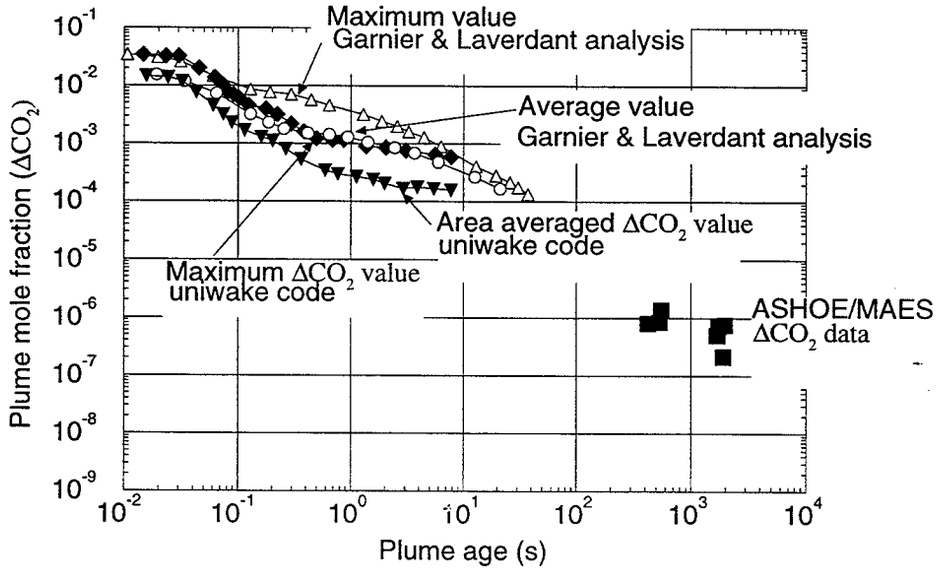

Figure 12: Axial plume mole fraction (CO_2) of Concorde supersonic aircraft. Comparison of two analyses with the ASHOE/MAES experimental data : UNIWAKE analysis and the present approach.